Cite this: DOI: 10.1039/c0xx00000x

www.rsc.org/xxxxxx

ARTICLE TYPE

A New Crystal: Layer-Structured Rhombohedral In_3Se_4

Guang Han,[a] Zhi-Gang Chen,*[a,d] Chenghua Sun,*[b] Lei Yang,[a] Lina Cheng,[a] Zhifeng Li,[e] Wei Lu,[e] Zachary M. Gibbs,[f] G. Jeffery Snyder,[d] Kevin Jack,[c] John Drennan,[c] Jin Zou*[a,c]

Received (in XXX, XXX) Xth XXXXXXXXX 20XX, Accepted Xth XXXXXXXXX 20XX

DOI: 10.1039/b000000x

A new layer-structured rhombohedral In_3Se_4 crystal was synthesized by a facile and mild solvothermal method. Detailed structural and chemical characterizations using transmission electron microscopy, coupled with synchrotron X-ray diffraction analysis and Rietveld refinement, indicate that In_3Se_4 crystallizes in a layered rhombohedral structure with lattice parameters of a = 3.964 ±0.002 Å and c = 39.59 ±0.02 Å and a space group: $R\bar{3}m$, and with a layer composition of Se-In-Se-In-Se-In-Se. The theoretical modeling and experimental measurements indicate that the In_3Se_4 is a self-doped n-type semiconductor. This study not only enriches the understanding on crystallography of indium selenide crystals, but also paves a way in the search for new semiconducting compounds.

1. Introduction

Layer-structured indium selenides, such as In_4Se_3, α/β-In_2Se_3, and β/γ-InSe, have attracted extensive attention in recent years due to their potential applications in thermoelectrics,[1-5] solar cells,[6] Li-ion batteries,[7, 8] photodetectors,[9-12] and memory devices.[13, 14] Specifically, In_4Se_3 forms a layered structure of $(In_3)^{5+}$ multivalent clusters bonded to Se ions,[1] while for α/β-In_2Se_3 and β/γ-InSe, atomic layers consisting of Se-In-Se-In-Se[10] and Se-In-In-Se,[7] respectively, are formed. These anisotropic bonding characteristics, including strong intralayer covalent bonding and weak interlayer van der Waals interactions, give rise to highly anisotropic optical, electrical, and thermal properties.[10, 11, 15, 16] In particular, the layered indium selenide nanomaterials are anticipated to exhibit superior physical properties, owing to their anisotropic photon geometries and large surface-to-volume ratios, together with photon and carrier confinement effects.[10] Once realized, such excellent properties will open up an opportunity for the application of layered indium selenide nanostructures in the next-generation nanoscale optical, electrical, and optoelectronic devices.

Bandgap is a key characteristic of the physical properties of materials that in turn affect their practical applications. Figure 1 summarizes the reported bandgaps for various indium selenides and indium tellurides. While most compositions, including InSe/InTe, In_2Se_3/In_2Te_3, and tetragonal (t-) In_3Te_4, show gaps greater than 1 eV, only In_4Se_3 and In_4Te_3 exhibit relatively narrow bandgaps of ~0.65 eV and ~0.5 eV, respectively.[17, 18] In contrast, the bandgaps of rhombohedral (r-) In_3Te_4 and In_3Se_4 are not known. Furthermore, although In_3Te_4 can be existed in rhombohedral or tetragonal crystal structures,[18, 19] the crystal structure of In_3Se_4 has not been found. In the case of r-In_3Te_4 with a layer structure consisting of Te-In-Te-In-Te-In-Te, superconductivity at 1.25 K has been observed,[19] indicating that r-In_3Se_4, if it could be synthesized, might possess new physical properties. Hence, it is highly desirable to synthesize r-In_3Se_4 and to explore its physical properties. The fact that its analogous structure, r-In_3Te_4, can only be synthesized under extreme condition (high pressure of ~3.5 GPa)[19] suggests that synthesis of a pure r-In_3Se_4 phase might be extremely difficult. Among all the available synthetic methods, solution-phase synthesis is a powerful approach to synthesize inorganic nanostructures of stable and metastable phases,[20-27] and several new and metastable In- and/or Se-containing phases[28-34] have been successfully synthesized recently through this approach by controlling the growth kinetics.

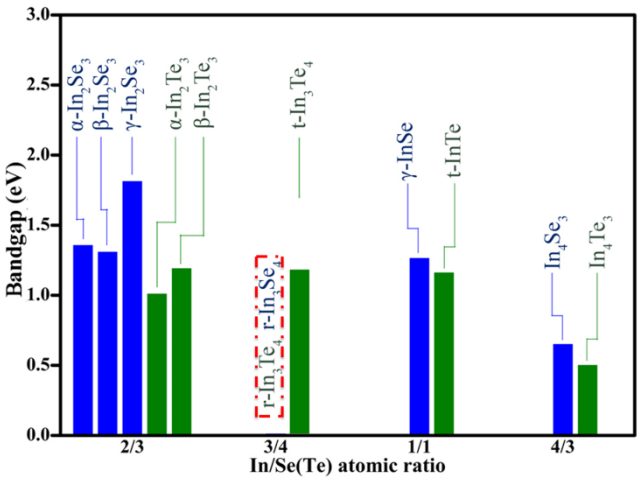

Figure 1 Experimental bandgaps of typical indium selenides and indium tellurides (α, β, and γ represent the commonly used names for the different phases of indium selenides and indium tellurides, and r- and t- stand for rhombohedral and tetragonal, respectively).

In this study, we demonstrate our successful synthesis of layered

r-In_3Se_4 flower-like nanostructures assembled in nanosheets using a mild and controllable solvothermal method. Through detailed characterization and theoretical modeling, it has been found that our synthesized In_3Se_4 is a new rhombohedral phase with lattice parameters of a = 3.964 ± 0.002 Å and c = 39.59 ± 0.02 Å, and a space group of R$\bar{3}$m, and it is a self-doped n-type semiconductor with an optical gap of ~0.55eV.

2. Experimental section

2.1 Materials synthesis

For a typical preparation of the nanostructured In_3Se_4, a certain amount of diluted NaHSe solution (0.1 mol/L, 3-6 ml) was swiftly injected into a mixed solvent (~40 ml) of ethylene glycol and deionised water with dissolved $InCl_3$ $4H_2O$ (0.01 mol/L) and ethylene diamine tetraacetic acid (EDTA) (~0.043 mol/L). After stirring for ~2 min, the solution was transferred into a Teflon-lined autoclave which was sealed and annealed at 200-230 ℃ for 24 h. The reacted product was collected by centrifuge, washed with deionised water and absolute ethanol for several times, and then dried for 12 h at 60 ℃.

2.2 Materials characterizations

The morphology of synthesized products was investigated by scanning electron microscopy (SEM, JEOL 6300, operated at 5 kV), and their structural and chemical characteristics were characterized by transmission electron microscopy (TEM, Philips FEI Tecnai F20, operated at 200 kV and equipped with energy-dispersive spectroscopy (EDS) for compositional analysis). Phase identification of synthesized products (loaded in a quartz capillary) at room temperature and elevated temperatures was performed by synchrotron powder diffraction using X-ray with a wavelength of 0.999977 Å on the powder diffraction beamline at the Australian Synchrotron. To determine the crystal structure of the synthesized products, Rietveld refinements on the synchrotron XRD pattern were carried out using the DIFFRAC^{plus} TOPAS 4.1 software.[35] The optical absorption spectrum of synthesized products was measured by Nicolet 6700 FTIR spectrometer at room temperature. The electrical resistivity and Hall coefficient of cold-pressed disc of synthesized products were measured by the Van de Pauw method, and the Hall carrier density was then calculated based on the measured Hall coefficient.[36, 37]

2.3 Computational methods

Spin-polarized density functional theory (DFT) calculation was carried out to optimize the lattice of In_3Se_4 within the generalized-gradient approximation,[38] together with the exchange-correlation functional of Perdew-Burke-Ernzerhof.[39, 40] This was implemented in the Vienna ab initio simulation package,[41, 42] in which the reciprocal space was spanned with a plane-wave basis with a kinetic energy cutoff of 550 eV.

3. Results and discussions

Figures 2a and 2b are typical SEM and TEM images of synthesized products, and clearly reveal that hierarchical flower-like structures with an overall diameter of 1-3 μm are assembled from nanosheets with a thickness of 20-40 nm. EDS analysis showed that these flower-like structures are composed of In and Se with an In:Se atomic ratio close to 3:4. Figure 2c shows a schematic illustration of the morphological characteristics of the nanostructures, and indicates the possibility of determining their crystal structure using selected area electron diffractions (SAED) taken along the normal to the nanosheet (beam direction 1) and along the nanosheet (beam direction 2). Figures 2d and 2e are typical SAED patterns with the incident electron beam normal to a nanosheet (beam direction 1) and parallel to a nanosheet (beam direction 2), respectively. Figures 2f and 2g are their respective corresponding schematic SAED patterns, from which, typical rhombohedral diffraction patterns can be clearly demonstrated. Based on this, the diffraction spots in the two SAED patterns can be indexed (the reflections satisfy the condition of –h + k + l = 3n with n = integer), and their zone axes can be determined as [0001] and [01$\bar{1}$0], respectively. To precisely determine the lattice parameters using SAED, a ~20 nm thick polycrystalline Au (with a well-known lattice parameter) thin film was coated on the TEM specimen as a reference, which allow $d_{11\bar{2}0}$ = 2.0 ± 0.1 Å and d_{0003} = 13.2 ± 0.1 Å to be determined. Therefore, the lattice parameters of synthesized indium selenide can be determined as a = 4.0 ± 0.2 Å and c = 39.7 ± 0.3 Å. Figures 2h and 2i are the corresponding high-resolution TEM images, in which the lattice spacings of 3.4 Å ($d_{10\bar{1}1}$) and 13.2 Å (d_{0003}) can be observed. It should be noted that the determined lattice parameters of our indium selenide structure are similar to those of r-X_3Y_4 compounds, including In_3Te_4 (space group R$\bar{3}$m, a = 4.26 Å, c = 40.6 Å)[17] and Bi_3Se_4 (space group R$\bar{3}$m, a = 4.23 Å, c = 40.5 Å).[17] This similarity strongly indicates that the synthesized indium selenide belongs to In_3Se_4 with a space group of R$\bar{3}$m.

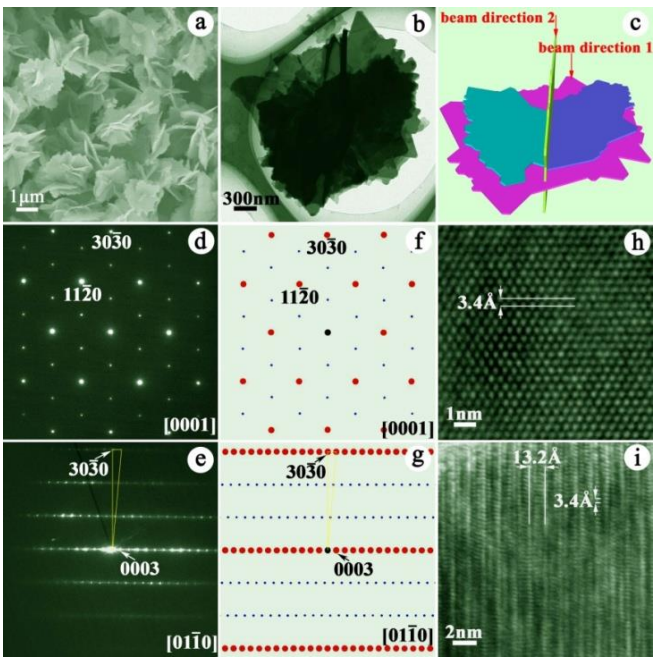

Figure 2 Structural characterization of the indium selenide nanostructures by electron microscopy: (a) and (b) typical SEM and TEM images; (c) a structural model based on these images defining the directions used for the SAED; (d) and (e) SAED patterns along zone axes [0001] and [01$\bar{1}$0], respectively; (f) and (g) schematic SAED patterns along [0001] and [01 $\bar{1}$ 0] zone axes, respectively; and (h) and (i) HRTEM images corresponding to the SAED patterns in (d) and (e), respectively.

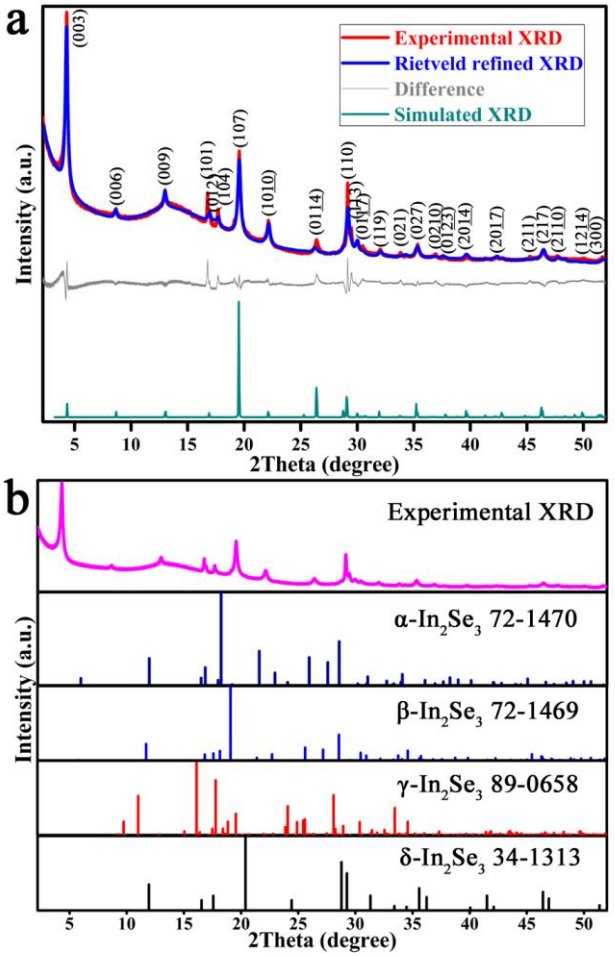

Figure 3 (a) Experimental synchrotron, Rietveld refined, and simulated XRD patterns of r-In_3Se_4 (The hump in the experimental pattern is due to the quartz capillary used to hold the samples), (b) Comparison between the experimental XRD pattern of r-In_3Se_4 and several diffraction peaks of various In_2Se_3 phases.

To further confirm the crystal structure of synthesized indium selenide, the synchrotron XRD was performed and result is shown as the red plot in Figure 3a. In Figure 3b, several standard diffraction profiles of different In_2Se_3 phases, including α, β, γ, and δ-In_2Se_3 phases are shown and none of them fits with the synchrotron XRD pattern. It is of interest to note that this synchrotron XRD pattern cannot be indexed by any other existing phase, but can be well indexed by a rhombohedral structure with lattice parameters of a = 4.0 ± 0.2 Å and c = 39.7 ± 0.3 Å. Using this set of lattice parameters and crystal system determined from TEM characterization, together with the atomic coordinates and symmetry of the analogous r-In_3Te_4, the crystal structure of r-In_3Se_4 crystal can be optimized and simulated using the spin-polarized density functional theory,[40] and the theoretical XRD pattern can be simulated. The green plot shown in Figure 3a is such a simulated XRD pattern, which shows an excellent agreement with the synchrotron XRD pattern (refer to the positions of the diffraction peaks). To further determine the atomic coordinates and refine its lattice parameters, Rietveld refinement on the synchrotron XRD pattern was carried out by using the simulated crystal structure of In_3Se_4 as the starting model. The refined XRD pattern and the discrepancy profile (generated by comparing the experimental XRD pattern and refined XRD pattern) are shown in Figure 3a as respectively blue and gray plots, and the refined atomic coordinates are listed in Table 1. The relatively low Rwp of 4.75% indicates the high reliability of the refinement; which in turn supports the synthesized In_3Se_4 to have a rhombohedral structure with lattice parameters of a = 3.964 ± 0.002 Å and c = 39.59 ± 0.02 Å, as well as a space group of R$\bar{3}$m.

Table 1. Crystallographic data of In_3Se_4 obtained by Rietveld refinement of the synchrotron XRD pattern

Site	Wyckoff Symbol	Symmetry	x	y	z	Occupation
In1	3a	$\bar{3}$m	0.0000	0.0000	0.0000	1
In2	6c	3m	0.0000	0.0000	0.4150(1)	1
Se1	6c	3m	0.0000	0.0000	0.1242(1)	1
Se2	6c	3m	0.0000	0.0000	0.3012(1)	1

Based on the above experimental evidences, the atomic model of r-In_3Se_4 can be built, as illustrated in Figure 4a, which shows that the In_3Se_4 belongs to a layered structure with layers consisting of Se-In-Se-In-Se-In-Se and each unit cell being constructed by three such layers along its [0001] direction. We note that the In-Se distances in our r-In_3Se_4 crystals are close to those of semiconducting β-In_2Se_3 (lattice parameters: a = 4.05 Å, c = 29.41 Å, space group: R$\bar{3}$m, and In atoms locate in the center of octahedral cages - formed by 6 adjacent Se atoms, as illustrated in Figure 4b),[43] indicating In^{+3} for the octahedrally coordinated In in our r-In_3Se_4.

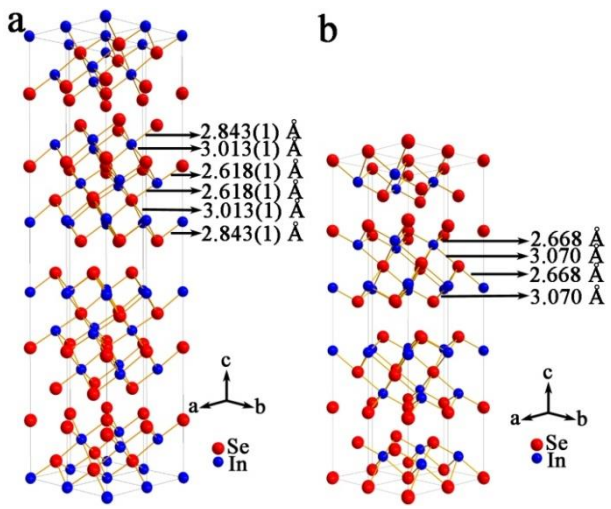

Figure 4 Crystal structure models of (a) r-In_3Se_4 and (b) β-In_2Se_3 with In-Se bond lengths labelled.

It should be noted that similar solvothermal syntheses have produced In_2Se_3 phases.[23, 27] In our experiments, EDTA was used to synthesize the indium selenide nanomaterials, from which In_3Se_4 nanostructures were secured. Therefore, the addition of EDTA has played a key role in the formation of In_3Se_4. We anticipate that EDTA can act as the template for the growth of two-dimensional In-Se layers in our solvothermal system.

To explore the intrinsic properties of this new indium selenide phase, the electronic structure of perfect In_3Se_4 crystal was calculated. Given the fact that the standard DFT may fail to describe the bandgap,[44] state-of-the-art calculations with hybrid

functional HSE06 was performed.[39-41, 45, 46] Figures 5a and 5b show the calculated band structure and the density of states of r-In_3Se_4 crystal. Clearly, the Fermi energy (dash line) is across several bands, indicating that the In_3Se_4 crystal may be metallic or a heavily doped n-type semiconductor. Since as mentioned early, In^{+3} should be the case for the octahedrally coordinated In in r-In_3Se_4, stoichiometric In_3Se_4 should have one extra electron per formula unit resulting in a heavily self-doped n-type semiconductor,[47] which is much like the case of La_3Te_4.[48]

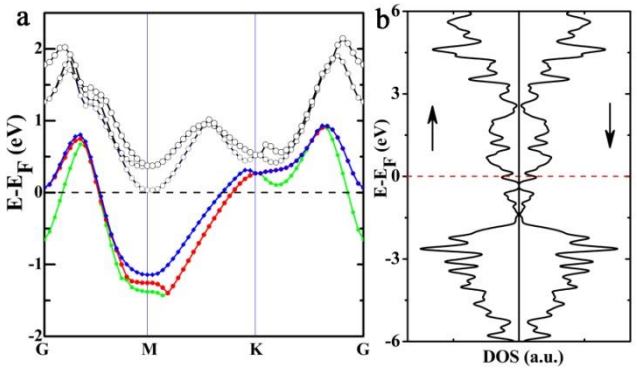

Figure 5 Calculated (a) band structures and (b) density of states, both for r-In_3Se_4 (the dash line shows the Fermi level at $E-E_F = 0$ eV).

To clarify the physical feature of our r-In_3Se_4, we performed optical absorption analysis and electrical property measurement. Figure 6a is an infrared optical absorption profile of our In_3Se_4 nanostructures, and shows its increasing with energy above ~0.55 eV which is a characteristic of a semiconductor. Figure 6b is the measured electrical resistivity of a typical cold-pressed In_3Se_4 disc as a function of temperature, and shows a decreasing resistivity with increasing the temperature, indicating again its semiconducting nature. Based on the measured Hall efficient, the carrier density (n_e) of our In_3Se_4 nanostructures can be determined to be $n_e \approx -1\times10^{-17}$ cm^{-3}, dominated by electrons, at room temperature, so that our In_3Se_4 nanostructures are n-type semiconductors.

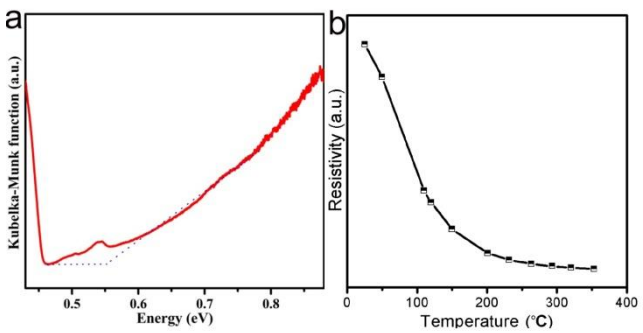

Figure 6 (a) Optical absorption spectrum of the In_3Se_4 flower-like nanostructures, (b) Resistivity of the cold-pressed In_3Se_4 disc.

Since the stability of a material is an important parameter for its applications, it is necessary to evaluate the stability of our synthesized In_3Se_4 nanostructures. In this regard, *in-situ* high-temperature synchrotron XRD analysis was performed and it has been found that the structure of our In_3Se_4 remains stable up to 800 ℃ (Figure 7), indicating that our In_3Se_4 has a high thermal stability, much higher than other layered indium selenide structures. Therefore, our In_3Se_4 nanostructures can be used in the high temperature environments.

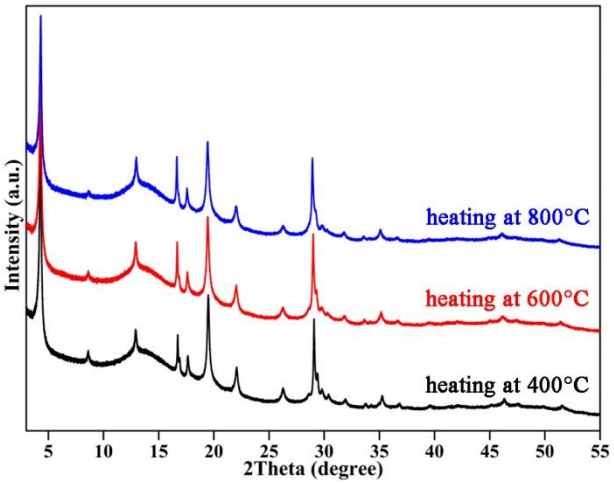

Figure 7 *In-situ* synchrotron XRD patterns of In_3Se_4 heated at various temperatures.

4. Conclusions

In summary, a mild and controllable solvothermal method has been developed for the synthesis of r-In_3Se_4 with high thermal stability. This new phase is confirmed to belong to a layered rhombohedral crystal structure (lattice parameters of $a = 3.964 \pm 0.002$ Å and $c = 39.59 \pm 0.02$ Å, and a space group of $R\bar{3}m$), in which layers consist of alternating Se-In-Se-In-Se-In-Se and stack along [0001] direction. The detailed computational calculations and experimental measurements reveal that our r-In_3Se_4 is a self-doped n-type semiconductor with an optical gap of ~0.55 eV. This study has deepened the understanding on crystallography of indium selenides and provided a new way for searching new semiconducting compounds.

ACKNOWLEDGMENT

This study is supported by the Australian Research Council, the QLD smart state future fellowship (Z.-G. C) and international fellowships (Z.-G. C./J. Z.); a UQ research foundation excellent award (Z.-G. C); and the CAS/SAFEA international partnership program for creative research teams. Australian Microscopy & Microanalysis Research Facility and Australian Synchrotron are acknowledged for providing characterization facilities for this study. We also appreciate the generous grants of CPU time from The University of Queensland and the Australian National Computational Infrastructure Facility.

Notes and references

[a] *Materials Engineering,* [b] *Australian Institute for Bioengineering and Nanotechnology, and* [c] *Centre for Microscopy and Microanalysis, The University of Queensland, Brisbane, QLD 4072, Australia. E-mail: j.zou@uq.edu.au, z.chen1@uq.edu.au, c.sun1@uq.edu.au*
[d] *Materials Science, California Institute of Technology, Pasadena, California 91124, USA.*
[e] *National Laboratory of Infrared Physics, Shanghai Institute of Technical Physics, Chinese Academy of Sciences, 500 Yutian Road, Shanghai 200083, China.*

[f] *Division of Chemistry and Chemical Engineering, California Institute of Technology, Pasadena, California 91124, USA.*

1. J.-S. Rhyee, K. H. Lee, S. M. Lee, E. Cho, S. I. Kim, E. Lee, Y. S. Kwon, J. H. Shim and G. Kotliar, *Nature*, 2009, **459**, 965.
2. J.-S. Rhyee, K. Ahn, K. H. Lee, H. S. Ji and J.-H. Shim, *Adv. Mater.*, 2011, **23**, 2191.
3. X. Shi, J. Y. Cho, J. R. Salvador, J. Yang and H. Wang, *Appl. Phys. Lett.*, 2010, **96**, 162108.
4. G. H. Zhu, Y. C. Lan, H. Wang, G. Joshi, Q. Hao, G. Chen and Z. F. Ren, *Phys. Rev. B*, 2011, **83**, 115201.
5. Z. G. Chen, G. Han, L. Yang, L. N. Cheng and J. Zou, *J. Prog. Nat. Sci. Mater. Int.*, 2012, **22**, 535.
6. J. Martine-Pastor, A. Segura, J. L. Valdes and A. Chevy, *J. Appl. Phys.*, 1987, **62**, 1477.
7. C. Julien, E. Hatzikraniotis, A. Chevy and K. Kambas, *Mater. Res. Bull.*, 1985, **20**, 287.
8. C. Julien, A. Khelfa, N. Benramdane, J. P. Guesdon, P. Dzwonkowski, I. Samaras and M. Balkanski, *Mater. Sci. Eng. B*, 1994, **23**, 105.
9. J.-J. Wang, F.-F. Cao, L. Jiang, Y.-G. Guo, W.-P. Hu and L.-J. Wan, *J. Am. Chem. Soc.*, 2009, **131**, 15602.
10. T. Zhai, X. Fang, M. Liao, X. Xu, L. Li, B. Liu, Y. Koide, Y. Ma, J. Yao, Y. Bando and D. Golberg, *ACS Nano*, 2010, **4**, 1596.
11. T. Zhai, Y. Ma, L. Li, X. Fang, M. Liao, Y. Koide, J. Yao, Y. Bando and D. Golberg, *J. Mater. Chem.*, 2010, **20**, 6630.
12. Q. L. Li, Y. Li, J. Gao, S. D. Wang and X. H. Sun, *Appl. Phys. Lett.*, 2011, **99**, 243105.
13. X. Sun, B. Yu, G. Ng, T. D. Nguyen and M. Meyyappan, *Appl. Phys. Lett.*, 2006, **89**, 233121.
14. B. Yu, S. Ju, X. Sun, G. Ng, T. D. Nguyen, M. Meyyappan and D. B. Janes, *Appl. Phys. Lett.*, 2007, **91**, 133119.
15. H. Peng, D. T. Schoen, S. Meister, X. F. Zhang and Y. Cui, *J. Am. Chem. Soc.*, 2007, **129**, 34.
16. H. Peng, C. Xie, D. T. Schoen and Y. Cui, *Nano Lett.*, 2008, **8**, 1511.
17. SpringerMaterials The Landolt-Börnstein Database, 2013.
18. G. A. Gamal, M. A. Abouzied and M. F. Sanaa, *Turk. J. Phys.*, 2012, **36**, 31.
19. S. Geller, A. Jayaraman and G. W. Hull Jr, *J. Phys. Chem. Solids*, 1965, **26**, 353.
20. J. A. Hollingsworth, D. M. Poojary, A. Clearfield and W. E. Buhro, *J. Am. Chem. Soc.*, 2000, **122**, 3562.
21. K. H. Park, K. Jang, S. Kim, H. J. Kim and S. U. Son, *J. Am. Chem. Soc.*, 2006, **128**, 14780.
22. S. Yang and D. F. Kelley, *J. Phys. Chem. B*, 2005, **109**, 12701.
23. X. Tan, J. Zhou and Q. Yang, *CrystEngComm*, 2011, **13**, 2792.
24. W. W. Zhou, Z. Y. Yin, D. H. Sim, H. Zhang, J. Ma, H. H. Hng and Q. Y. Yan, *Nanotechnology*, 2011, **22**, 195607.
25. L. Cheng, Z.-G. Chen, S. Ma, Z.-D. Zhang, Y. Wang, H.-Y. Xu, L. Yang, G. Han, K. Jack, G. Lu and J. Zou, *J. Am. Chem. Soc.*, 2012, **134**, 18920.
26. P. Liu, S. Yu, W. Fan and W. Shi, *Dalton Trans.*, 2013, **42**, 2887.
27. W. Shi, S. Yu, P. Liu, W. Fan, H. Luo and S. Song, *Chem. Eng. J.*, 2013, **225**, 474.
28. M. T. Ng, C. B. Boothroyd and J. J. Vittal, *J. Am. Chem. Soc.*, 2006, **128**, 7118.
29. D. Pan, L. An, Z. Sun, W. Hou, Y. Yang, Z. Yang and Y. Lu, *J. Am. Chem. Soc.*, 2008, **130**, 5620.
30. M. E. Norako, M. J. Greaney and R. L. Brutchey, *J. Am. Chem. Soc.*, 2012, **134**, 23.
31. J.-J. Wang, Y.-Q. Wang, F.-F. Cao, Y.-G. Guo and L.-J. Wan, *J. Am. Chem. Soc.*, 2010, **132**, 12218.
32. Y. Qi, Q. Liu, K. Tang, Z. Liang, Z. Ren and X. Liu, *J. Phys. Chem. C*, 2009, **113**, 3939.
33. M. E. Norako, M. A. Franzman and R. L. Brutchey, *Chem. Mater.*, 2009, **21**, 4299.
34. M. E. Norako and R. L. Brutchey, *Chem. Mater.*, 2010, **22**, 1613.
35. DIFFAC^{plus} TOPAS 4, Bruker AXS GmbH, Karlsruhe, Germany, 2008.
36. L. Cheng, Z.-G. Chen, L. Yang, G. Han, H.-Y. Xu, G. J. Snyder, G.-Q. Lu and J. Zou, *J. Phys. Chem. C*, 2013, **117**, 12458.
37. K. A. Borup, E. S. Toberer, L. D. Zoltan, G. Nakatsukasa, M. Errico, J. P. Fleurial, B. B. Iversen and G. J. Snyder, *Rev. Sci. Instrum.*, 2012, **83**.
38. W. Kohn and L. J. Sham, *Phys. Rev.*, 1965, **140**, A1133.
39. J. P. Perdew, K. Burke and M. Ernzerhof, *Phys. Rev. Lett.*, 1996, **77**, 3865.
40. G. Kresse and D. Joubert, *Phys. Rev. B*, 1999, **59**, 1758.
41. G. Kresse and J. Furthmüller, *Phys. Rev. B*, 1996, **54**, 11169.
42. G. Kresse and J. Furthmuller, *Comput. Mater. Sci.*, 1996, **6**, 15.
43. K. Osamura, Y. Murakami and Y. Tomiie, *J. Phys. Soc. Japan*, 1966, **21**, 1848.
44. J. P. Perdew, *Int. J. Quantum Chem.*, 1985, **28**, 497.
45. P. E. Blöchl, *Phys. Rev. B*, 1994, **50**, 17953.
46. J. Heyd, G. E. Scuseria and M. Ernzerhof, *J. Chem. Phys.*, 2006, **124**, 219906.
47. E. S. Toberer, A. F. May and G. J. Snyder, *Chem. Mater.*, 2009, **22**, 624.
48. A. F. May, J.-P. Fleurial and G. J. Snyder, *Phys. Rev. B*, 2008, **78**, 125205.